# Supplementary Materials

# PremPRI: Predicting the Effects of Missense Mutations on Protein-RNA Interactions

Ning Zhang[1], Haoyu Lu[1], Yuting Chen[1], Zefeng Zhu[1], Qing Yang[1], Shuqing Wang[1] and Minghui Li[1,*]

[1]Center for Systems Biology, Department of Bioinformatics, School of Biology and Basic Medical Sciences, Soochow University, Suzhou 215123, China

*corresponding author, minghui.li@suda.edu.cn

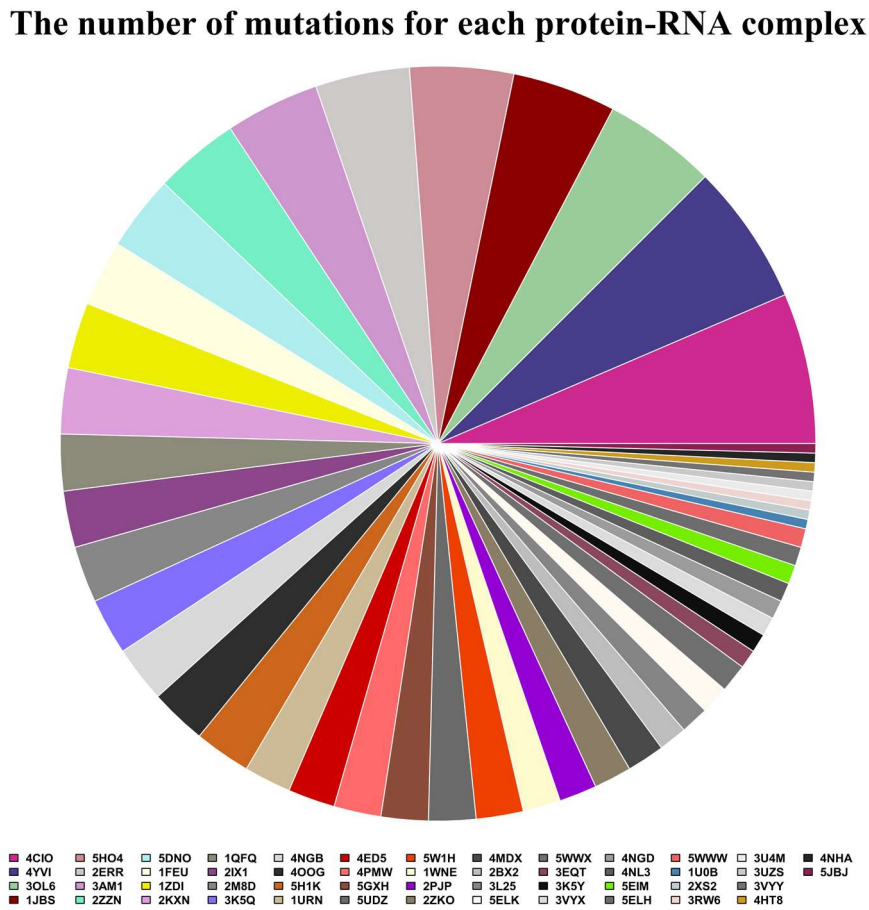


| # of mutations | PDB ID of complex |
|---|---|
| 16 | 4CIO |
| 15 | 4YVI |
| 12 | 3OL6 |
| 11 | 1JBS, 5HO4 |
| 10 | 2ERR, 3AM1 |
| 9 | 2ZZN |
| 8 | 5DNO |
| 7 | 1FEU, 1ZDI, 2KXN |
| 6 | 1QFQ, 2IX1, 2M8D, 3K5Q, 4NGB, 4OOG, 5H1K |
| 5 | 1URN, 4ED5, 4PMW, 5GXH, 5UDZ, 5W1H |
| 4 | 1WNE, 2PJP, 2ZKO, 4MDX |
| 3 | 2BX2, 3L25, 5ELK, 5WWX |
| 2 | 3EQT, 3K5Y, 3VYX, 4NGD, 4NL3, 5EIM, 5ELH, 5WWW |
| 1 | 1U0B, 2XS2, 3RW6, 3U4M, 3UZS, 3VYY, 4HT8, 4NHA, 5JBJ |

**Figure S1.** The number of mutations for each protein-RNA complex in S248 dataset, which includes 248 mutations from 50 protein-RNA complexes.

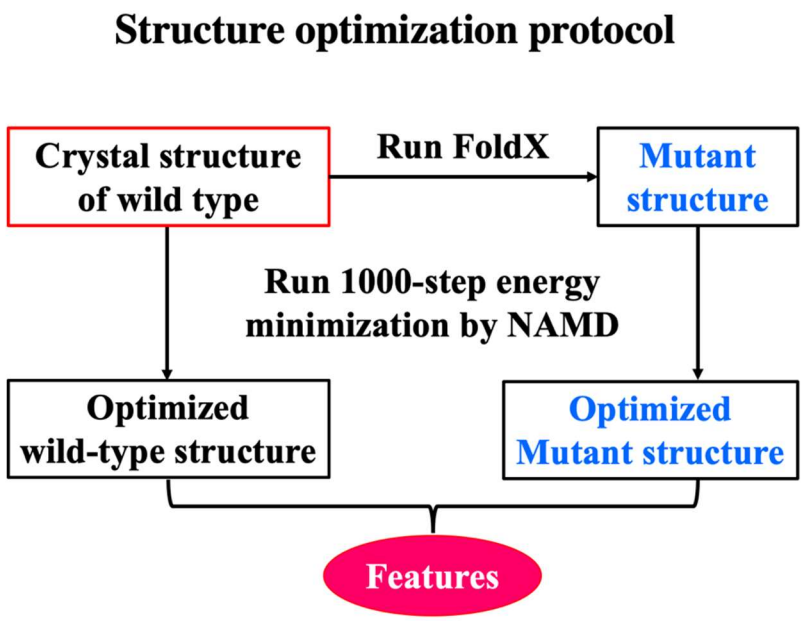


**Figure S2.** The flowchart of structure optimization protocol.

**a.** **b.**

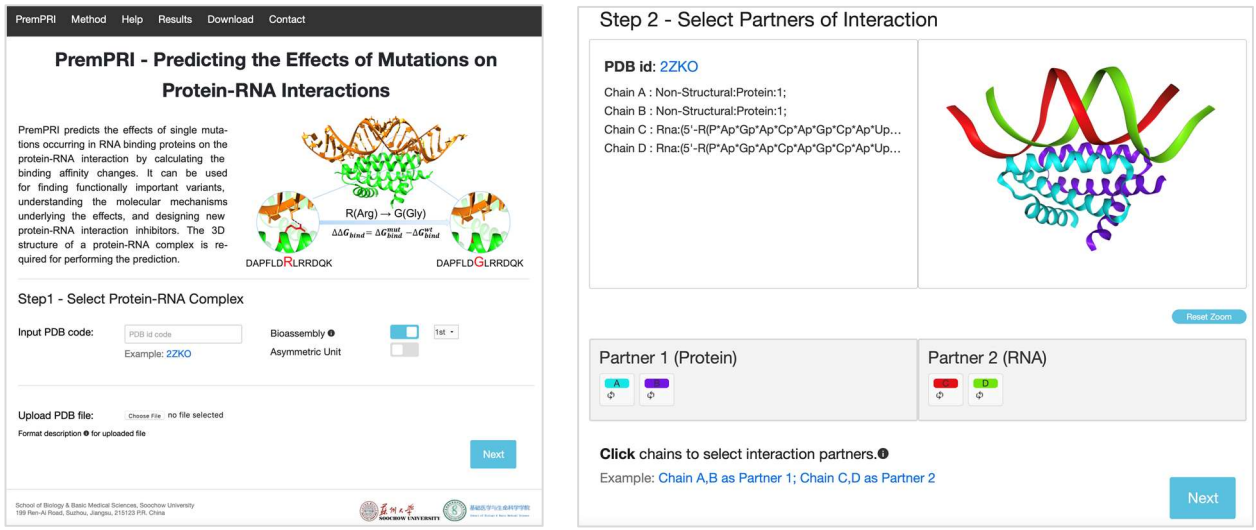


**c.**

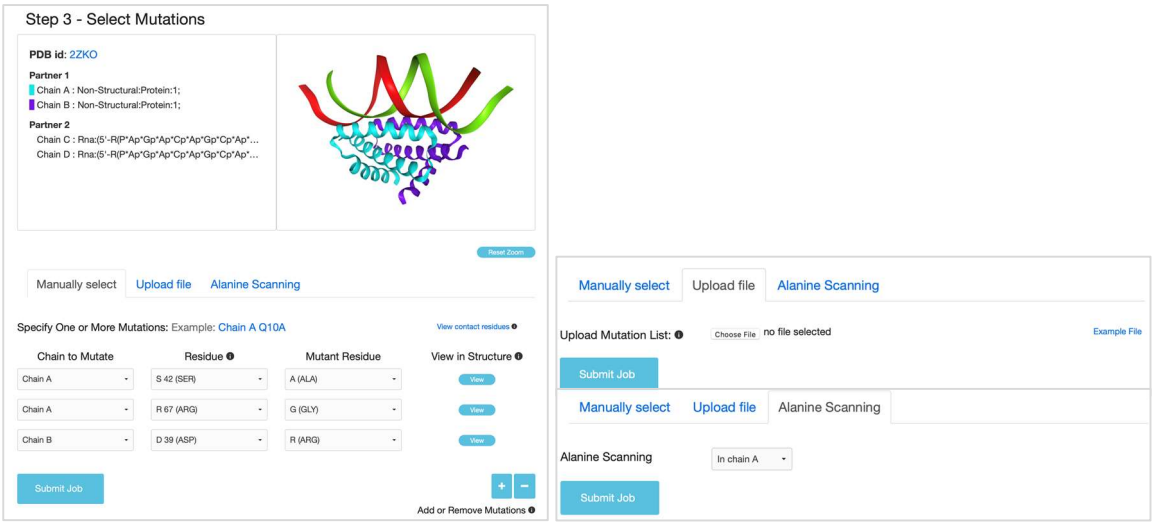


**Figure S3.** (a) The entry page of PremPRI server. (b) The second step for selecting interaction partners**.** (c) The third step for selecting mutations and three options are provided: "Specify One or More Mutations Manually", "Upload Mutation List" and "Alanine Scanning for Each Chain".

**a.**

**Job id:** 20200505040601737058075 92

- Summary

| PDB ID | Protein | RNA | Number of mutations | Start time (EST) | Processing time | Results |
|---|---|---|---|---|---|---|
| 2ZKO | A, B | C, D | 3 | 2020-05-04 23:09 | 5 min | Download |

- Results

| # | Mutated Chain | Mutation | ΔΔG | Interface? | Structure |
|---|---|---|---|---|---|
| 1 | A | S42A | **1.5** | Yes | Explore |
| 2 | A | R67G | **1.03** | No | Explore |
| 3 | B | D39R | **2.91** | Yes | Explore |

Click

**b.**

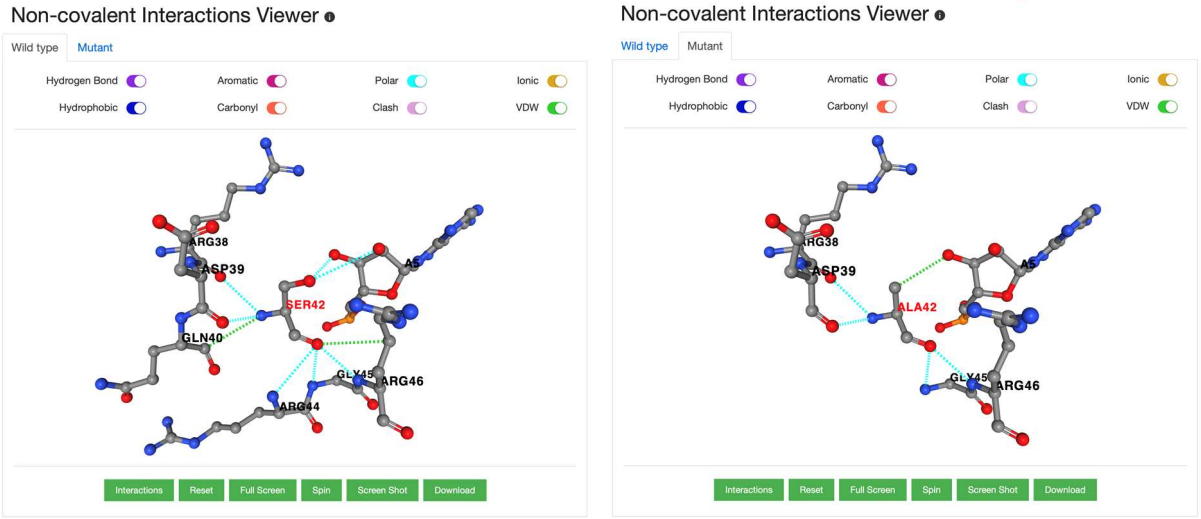


**Figure S4.** (a) The final results. "Processing time" refers to the running time of a job without counting the waiting time in the queue. (b) Interactive 3D viewer showing the non-covalent interactions between the mutated site in the NS1 protein of human influenza virus A (PDB ID: 2ZKO, mutation: S42A) and its adjacent residues/nucleotides in the wild-type (left) and mutant (right) complex respectively, generated by Arpeggio.

**Table S1. Experimental datasets used for training methods of PremPRI, mCSM-NA and PrabHot.**

| Dataset | # of mutations | # of complexes | Description |
|---|---|---|---|
| S248 | 248 | 50 | training set of PremPRI |
| S264 | 264(67) | 33(5) | training set of mCSM-NA including mutations from both protein-DNA and -RNA complexes; bracket: the number of mutations from protein-RNA complexes |
| S151 | 151 | 32 | training set of PrabHot, classification method |
| S16 | 16 | 2 | overlap mutations between S248 and S264 |
| S92 | 92 | 21 | overlap mutations between S248 and S151 |

**Different categories for mutations in S248**

| Category | # of mutations | # of complexes | Description |
|---|---|---|---|
| Alanine-scanning | 213 | 50 | substitutions of residues into alanine |
| Non-alanine-scanning | 35 | 13 | substitutions of residues into non-alanine |
| Interface | 154 | 45 | mutations occur at protein-RNA binding interface |
| Non-interface | 94 | 31 | mutations do not occur at binding interface |
| Protein-ssRNA | 122 | 24 | mutations occur in protein-single stranded RNA complexes |
| Protein-dsRNA | 126 | 26 | mutations occur in protein-double stranded RNA complexes |

**Table S2. The p-value and importance of each feature in multiple linear regression scoring function of PremPRI.** All Features have significant contribution to the quality of the model (p-value < 0.01, t-test). The features are ranked with respect to the importance.

| Feature | P-value | Importance |
|---|---|---|
| $\Delta P_{FWY}$ | 1.40E-13 | 0.52 |
| $N_{inter}$ | 7.24E-07 | 0.30 |
| $Closeness$ | 6.90E-06 | 0.30 |
| $R_{L/SA}$ | 1.23E-05 | 0.29 |
| $\Delta\Delta E_{vdw.re}$ | 1.18E-05 | 0.28 |
| $P_{coil}$ | 2.07E-05 | 0.26 |
| $\Delta\Delta E_{elec}$ | 1.49E-03 | 0.20 |
| $\Delta SA$ | 7.78E-04 | 0.19 |
| $\Delta P_{KR-DE}$ | 5.13E-04 | 0.19 |
| $\Delta OMH$ | 3.27E-03 | 0.19 |
| $\Delta\Delta E_{vdw}$ | 3.59E-03 | 0.15 |

Standardized coefficients are used for describing the importance.

**Table S3. The performance using multiple linear regression (MLR), Random Forest (RF), Back Propagation Neural Network (BPNN), Support Vector Machine (SVM) and eXtreme Gradient Boosting (XGBoost) algorithms to build PremPRI model, respectively.**

| Algorithm | Method | R | RMSE | Slope |
|---|---|---|---|---|
| **MLR** | PremPRI | 0.72 | 0.76 | 1.00 |
| | PremPRI (CV3) | 0.61 | 0.87 | 0.89 |
| **RF** | PremPRI | 0.70 | 0.79 | 1.21 |
| | PremPRI (CV3) | 0.46 | 0.98 | 1.15 |
| **BPNN** | PremPRI | 0.82 | 0.63 | 1.01 |
| | PremPRI (CV3) | 0.46 | 0.99 | 0.72 |
| **SVM** | PremPRI | 0.85 | 0.61 | 1.25 |
| | PremPRI (CV3) | 0.42 | 1.00 | 0.89 |
| **XGBoost** | PremPRI | 0.99 | 0.14 | 1.09 |
| | PremPRI (CV3) | 0.40 | 1.00 | 0.95 |

PremPRI: trained and tested on S248 dataset; PremPRI (CV3): leave-one-complex-out validation results.

R: Pearson correlation coefficient. RMSE (kcal $mol^{-1}$): root-mean-square error. Slope: the slope of the regression line between experimental and predicted $\Delta\Delta G$ values. All presented correlation coefficients are statistically significantly different from zero (p-value << 0.01, t-test).

**Table S4. Variance inflation factor (VIF) of each feature in PremPRI model.** The features are ranked with respect to the VIF. The VIF of each feature is less than three, indicating low collinear relationships among 11 independent variables.

| Feature | VIF |
|---|---|
| $\Delta P_{FWY}$ | 2.20 |
| $\Delta OMH$ | 2.13 |
| $R_{L/SA}$ | 2.12 |
| $Closeness$ | 2.07 |
| $\Delta\Delta E_{vdw.re}$ | 1.97 |
| $\Delta\Delta E_{elec}$ | 1.85 |
| $P_{coil}$ | 1.81 |
| $N_{inter}$ | 1.69 |
| $\Delta SA$ | 1.61 |
| $\Delta P_{KR-DE}$ | 1.41 |
| $\Delta\Delta E_{vdw}$ | 1.25 |

**Table S5. PremPRI performance for different categories of mutations.**

| Mutation category | Method | R | RMSE | Slope |
|---|---|---|---|---|
| **Alanine-scanning** | PremPRI | 0.71 | 0.74 | 1.01 |
| | PremPRI (CV3) | 0.61 | 0.83 | 0.89 |
| **Non-alanine-scanning** | PremPRI | 0.78 | 0.85 | 0.98 |
| | PremPRI (CV3) | 0.60 | 1.08 | 0.90 |
| **Interface** | PremPRI | 0.75 | 0.78 | 1.05 |
| | PremPRI (CV3) | 0.62 | 0.93 | 0.93 |
| **Non-interface** | PremPRI | 0.65 | 0.71 | 0.86 |
| | PremPRI (CV3) | 0.58 | 0.77 | 0.76 |
| **Protein-ssRNA** | PremPRI | 0.76 | 0.82 | 1.08 |
| | PremPRI (CV3) | 0.61 | 0.98 | 0.99 |
| **Protein-dsRNA** | PremPRI | 0.64 | 0.69 | 0.84 |
| | PremPRI (CV3) | 0.59 | 0.75 | 0.74 |

PremPRI: trained and tested on S248 dataset; PremPRI (CV3): leave-one-complex-out validation results.

R: Pearson correlation coefficient. RMSE (kcal $mol^{-1}$): root-mean-square error. Slope: the slope of the regression line between experimental and predicted $\Delta\Delta G$ values. All presented correlation coefficients are statistically significantly different from zero (p-value << 0.01, t-test).

**Table S6. Average weighting coefficient and the corresponding standard deviation (in bracket) for each feature in three types of cross-validation (CV1-CV3). The weighting coefficient in the PremPRI model is presented for the comparison.** The features are ranked with respect to the absolute value of weighting coefficient in the PremPRI model.

| Feature | CV1 | CV2 | CV3 | PremPRI |
|---|---|---|---|---|
| $\Delta P_{FWY}$ | -218.13(31.43) | -216.40(15.44) | -215.51(9.57) | -216.23 |
| $R_{L/SA}$ | 83.93(17.89) | 83.01(10.69) | 83.53(4.26) | 83.51 |
| $\Delta P_{KR-DE}$ | -31.65(16.34) | -32.70(7.45) | -33.34(3.73) | -33.48 |
| $Closeness$ | 5.59(1.33) | 5.66(0.77) | 5.77(0.31) | 5.77 |
| $P_{coil}$ | -5.95(1.68) | -5.71(0.81) | -5.66(0.44) | -5.67 |
| $\Delta OMH$ | 0.21(0.06) | 0.21(0.03) | 0.21(1.42E-02) | 0.21 |
| $\Delta\Delta E_{vdw.re}$ | -0.11(2.57E-02) | -0.11(1.19E-02) | -0.11(5.31E-03) | -0.11 |
| $\Delta\Delta E_{vdw}$ | 0.02(6.90E-03) | 0.02(3.81E-03) | 0.02(1.20E-03) | 0.02 |
| $N_{inter}$ | -9.55E-03(2.01E-03) | -9.27E-03(7.24E-04) | -9.21E-03(4.41E-04) | -9.20E-03 |
| $\Delta SA$ | 5.47E-03(1.70E-03) | 5.56E-03(9.66E-04) | 5.52E-03(3.34E-04) | 5.54E-03 |
| $\Delta\Delta E_{elec}$ | 1.07E-03(3.66E-04) | 1.16E-03(1.72E-04) | 1.14E-03(3.90E-05) | 1.14E-03 |
| **Intercept** | -0.33(0.54) | -0.39(0.30) | -0.41(0.14) | -0.41 |

**Table S7. Comparison of methods' performances on three mutations from TthL1–RNA complex.** $\Delta\Delta G_{exp}$ and $\Delta\Delta G_{pred}$ are experimentally determined and predicted binding affinity change (in kcal $mol^{-1}$), respectively.

| Mutation | $\Delta\Delta G_{exp}$ | PremPRI | mCSM-NA | FoldX | PrabHot |
|---|---|---|---|---|---|
| T217A | 2.49 | 1.32 | -1.18 | -1.22 | hotspot |
| T217V | 3.61 | 1.87 | 1.20 | 0.12 | hotspot |
| M218L | 6.58 | 1.67 | 1.59 | 0.13 | hotspot |
| G219V | 5.35 | 1.94 | -1.53 | 0.24 | non-hotspot |

Our training dataset of S248 includes one mutation of T217A from this complex, which was excluded from the training dataset when testing on this case.